Mo/HMCM-22 catalysts for methane dehydroaromatization: A multinuclear MAS NMR study

ARTICLE *in* THE JOURNAL OF PHYSICAL CHEMISTRY B · FEBRUARY 2001

Impact Factor: 3.3 · DOI: 10.1021/jp002011k

6 AUTHORS, INCLUDING:

Yuying Shu
W. R. Grace
48 PUBLICATIONS **1,456** CITATIONS
SEE PROFILE

Xiumei Liu
China University of Mining Technology
50 PUBLICATIONS **1,171** CITATIONS
SEE PROFILE

Yide Xu
Dalian Institute of Chemical Physics
122 PUBLICATIONS **4,324** CITATIONS
SEE PROFILE

Mo/HMCM-22 Catalysts for Methane Dehydroaromatization: A Multinuclear MAS NMR Study

Ding Ma, Yuying Shu, Xiuwen Han, Xiumei Liu, Yide Xu, and Xinhe Bao*

State Key Laboratory of Catalysis, Dalian Institute of Chemical Physics, Chinese Academy of Sciences, Dalian 116023, P.R. China

Received: June 2, 2000; In Final Form: September 19, 2000

Detailed NMR investigations on fresh and coked Mo/HMCM-22 catalysts for methane dehydro-aromatization were presented. ^{27}Al MAS and ^{29}Si MAS as well as corresponding CP/MAS NMR experiments have proved that an interaction between molybdenum and the zeolite lattice occurs during the impregnation and calcination processes of the catalysts. With Brönsted acid sites serving as a powerful trap, molybdenum migrates into the internal channels of the zeolite and reacts preferentially with bridging hydroxyls groups. Thus, molybdenum is anchored to the framework aluminum through an oxygen bridge, which, in turn, modifies the acidic properties of the HMCM-22 and leads to a high dispersion of the molybdenum. If this kind of interaction becomes stronger, expelling of aluminum from the zeolite lattice would occur, with the forming of both octahedral nonframework aluminum and $Al_2(MoO_4)_3$ crystallites. The latter can be hydrated to $[Al(OH)_n(H_2O)_{6-n}]_n(MoO_4)$ ($n = 1$ or 2) in a water-saturated desiccator and can give a line at ca. 14 ppm in the ^{27}Al MAS NMR spectrum. UV−Raman results suggest that the carbonaceous deposits on the catalysts are mainly hydrogen-deficient aromatic type, which are also verified by ^{1}H → ^{29}Si CP/MAS and ^{1}H → ^{27}Al CP/MAS NMR, as well as the failure for conducting the ^{13}C CP/MAS NMR experiment. ^{1}H → ^{27}Al CP/MAS NMR experiments indicate that most of the coke is deposited on framework aluminum (Brönsted site). Regeneration in an oxygen atmosphere leads to the formation of a considerable amount of $Al_2(MoO_4)_3$ crystallites. However, the catalytic activity can be properly restored after the regeneration; thus, the idea of taking this species as the detrimental factor for this reaction can be ruled out. On the other hand, lattice destruction of the zeolite is suggested to be responsible for the poor performance exhibited by the 10Mo/HMCM-22 catalyst. The synergic effect between molybdenum and Brönsted acid sites is considered to be the main reason for the outstanding catalytic performance of the 6Mo/HMCM-22 catalyst.

1. Introduction

The transformation of methane into useful chemical products was a hot topic in the last century, especially in those days after the petroleum crisis.[1] A main reason widely accepted is the consideration of natural gas (methane) as the potential resources for energy and chemical production in the 21st century.[2] So far, the efficient utilization, especially direct use, of methane is a great challenge to heterogeneous catalysis, from both practical and theoretical points of view. It is well-known that methane is such a stable molecule that its activation needs a harsh condition such as concentrated sulfuric acid[3] or strong basic metal oxide,[4] depending on different mechanisms concerned. In 1993, we reported that methane can be transformed into aromatics under a nonoxidative condition at 973 K and atmospheric pressure by using transition metal ion (TMI)-modified acidic solid materials, i.e., the proton form of molecular sieves.[5] Since then, this reaction/catalyst system has been investigated from various aspects.[6−17] It was found that the Mo/HZSM-5 catalyst is the best one among the vast numbers of catalysts tested, which can give a methane conversion of about 10% and benzene selectivity of 50−60% at 973 K.[7,9,17] Many researchers have pointed out that besides the Brönsted acid sites, the specific state of the molybdenum species (carbon-modified Mo_2C or MoO_xC_y) and the channel structure of the zeolite played a key role in methane activation and the succeeding aromatization.[5−7,9,12,18−20] Recent investigation by Ichikawa et al.[21,22] indicates that Re/HZSM-5 catalysts exhibit the methane conversion and benzene selectivity equivalent to or higher than Mo/HZSM-5. Coupling the addition of CO/CO_2 with reaction of methane aromtization, it will lead to a longer lifetime of the catalysts.[21,22]

TABLE 1: Catalytic Performance of Various Catalysts (Data Taken after 120 min Reaction)[a]

	C_{CH_4} (%)	selectivity of main products (%)		
		C_6H_6	$C_{10}H_8$	coke
6%Mo/HZSM-5	10.0	58.2	18.2	16.5
2%Mo/HMCM-22	6.6	55.6	7.1	29.9
6%Mo/HMCM-22	9.9	72.8	5.9	13.0
10%Mo/HMCM-22	7.1	55.2	3.4	37.1
regenerated 6%Mo/HMCM-22	9.2	74.2	4.7	13.5

[a] Reaction was conducted at 973 K and SV = 1500 mL/(g·h); the conversion of methane and selectivity of products are calculated according to the carbon number basis.

Recently, we have reported that a better catalytic performance of this reaction can be achieved on a HMCM-22 supported molybdenum catalyst.[23] It gives rise to a higher benzene yield (>7%, see Table 1) and has a longer lifetime (>48 h) as compared with that of Mo/HZSM-5. The particular feature of this catalyst is suggested to be attributed to the unique channel

10.1021/jp002011k CCC: $20.00
Published on Web 02/08/2001

structure of the MCM-22 zeolite. Its topological structure is composed of the interconnected $\{4^3 5^6 6^3 [4^3]\}$ building unit, forming two independent pore systems: two-dimensional ten-ring intralayer channels, and 12-ring interlayer supercages with a depth of 18.2 Å, both accessible through ten-ring apertures.[24−29] The zeolite has already shown specific characteristics in other catalytic reactions.[30] Probably, it is this kind of structure that leads to a different catalytic behavior.

At the same time, for bifunctional catalysts such as the one used in the present case, the problem of how the two components interact with each other needs to be clarified. This distribution/interaction will alter the whole catalytic performance if different preparation methods or different contents of one component are used. The application of MAS NMR in the characterization of the zeolite structure and in the investigation of the synergic effects in multiple-component catalyst systems have been widely recognized.[31] In this paper, high-resolution multinuclear MAS NMR techniques, such as ^{27}Al, ^{29}Si MAS and CP/MAS, ^{1}H MAS, and ^{1}H{^{27}Al} spin echo double resonance (SEDOR), were used for the structural characterization of the catalysts, so as to reveal the interaction between molybdenum species and HMCM-22 zeolite, especially that with the Brönsted acid sites. At the same time, the NMR profiles of the catalysts after deactivation (coking) are also presented. The structure−activity relationship of the catalysts is discussed.

2. Experimental Section

Materials. MCM-22 (Si/Al = 15) zeolite was synthesized according to the procedures described in the references using hexamethylenimine (HMI) as the directing agent.[24,25] The details of the synthesis have been illustrated elsewhere.[23] The crystalline structure (MWW) of the as-synthesized zeolites was evidenced by XRD (D/max-rB diffractometer using Cu Kα radiation), and no hybrid crystallites were observed. The proton form of the zeolite was obtained by exchanging three times the Na^+ by 1 M NH_4NO_3 solution and was washed and dried at 373 K, heated to 823 K at 10 K/min, and kept at 823 K for 4 h.

Mo/HMCM-22 catalysts were obtained by impregnating 10 g of HMCM-22 powder with 20 mL of the aqueous solution containing the desirable amount of ammonium heptamolybdate (AHM) and then dried at RT for 12 h. After the samples were further dried at 373 K for 8 h and calcined in air at 773 K for 5 h, they were crushed and sieved to 20-to-60-mesh granules for catalytic evaluation. Mo/HMCM-22 with different Mo loadings were denoted as *x*Mo/HMCM-22, where *x* is the nominal Mo content in weight percent. Prior to ^{27}Al MAS and ^{1}H → ^{27}Al CP/MAS NMR measurements, the samples were rehydrated completely in a desiccator containing saturated NH_4NO_3.[32]

MAS NMR. All the NMR spectra were obtained at 9.4 T on a Bruker DRX-400 spectrometer using 4 mm ZrO_2 rotors. ^{29}Si MAS NMR spectra were recorded at 79.5 MHz using a 0.8 μs ($\pi/8$) pulse with a 4 s recycle delay and 3000 scans. ^{1}H → ^{29}Si CP/MAS NMR experiments were performed with a 4 s recycle delay, 8000 scans, and a contact time of 1.5 ms. The magic angle spinning rate for all ^{29}Si spectra was 4 kHz, and chemical shifts were referenced to (4,4-dimethyl-4-silapentanesulfonato)-sodium (DSS). ^{27}Al MAS NMR spectra were recorded at 104.3 MHz using a 0.75 μs ($\pi/12$) pulse with a 3 s recycle delay and 800 scans. A 1% aqueous $Al(H_2O)_6^{3+}$ solution was used as the reference of chemical shifts, and samples were spun at 8 kHz. ^{1}H → ^{27}Al CP/MAS NMR measurements were recorded with a single contact of 1.2 ms duration, recycle delay of 3 s, and MAS at 10 kHz.[32,33] The Hartmann−Hahn condition was established in one scan on a sample of pure and highly crystalline kaolinite using similar acquisition parameters. Because only the central ($-1/2 \leftrightarrow +1/2$) transition is observed, excitation is selective and therefore the Hartmann−Hahn condition is $3\gamma_{Al}B_{Al} = \gamma_H B_H$, where γ_{Al} and γ_H denote the gyromagnetic ratios of ^{27}Al and ^{1}H, and B is the radio frequency field strength. To get a satisfactory signal-to-noise ratio, normally, 15 000−16 000 scans were accumulated. ^{1}H MAS NMR spectra were collected at 400.1 MHz using single-pulse experiments with $\pi/2$ pulse and a 4 s recycle delay. A [$\pi/2-\tau-\pi-\tau-$acquire] spin echo pulse ($\pi/2 = 4.5$ μs) was also used to acquire ^{1}H spectra and τ was set to one rotor period. Prior to the measurements, the samples were dehydrated at 673 K and 10^{-2} Pa for about 20 h in a homemade apparatus,[34] by which the treated sample can be filled in situ into a NMR rotor, sealed, and transferred to the spectrometer without exposure to air. ^{1}H{^{27}Al} SEDOR MAS NMR experiments were performed according to the method of Veeman et al.[35] In the experiments, a [$\pi/2-\tau-\pi-\tau-$acquire] spin echo pulse was applied to the ^{1}H channel and aluminum was irradiated simultaneously during the first τ period. All the ^{1}H spectra were accumulated for 200 scans and spun at 5 kHz. The chemical shifts were referenced to a saturated aqueous solution of DSS.

The ^{1}H{^{27}Al} spin echo double resonance experiment is conducted by making use of the passages that occur between the ^{27}Al Zeeman levels under the condition of slow rotation speed and continuous irradiation. This leads to an alteration of the evolution of the proton spins that are coupled to the quadrupolar ^{27}Al nuclei, and as a result, the proton spin is no longer refocused at the rotor echo. Thus, the intensity of the species that strongly coupled with aluminum will suffer in ^{1}H{^{27}Al} SEDOR MAS NMR experiments.[36]

UV−Raman Measurements. UV−Raman spectra were recorded on a homemade spectrometer,[37] which consisted of an intracavity frequency-doubled Ar^+ ion laser (Coherent, Innova 300 FRED), using a line at 257 nm as the excitation source, a three-grating spectrometer (Spex Triplemate 1877D) and a CCD detector (EG&G Co., Ltd.). The resolution of the Raman system was about 1.5 cm^{-1} (at 257 nm excitation) and the power of the 257 nm laser line at the sample was kept at about 2 mW to avoid overheating of the sample.

Catalytic Evaluation. The detailed catalytic evaluation method was described elsewhere.[17] In brief, a quartz tubular fixed-bed reactor with a 6.2 mm i.d. was used. Before introduction of the reactant, the catalyst was treated in helium (UHP) at 973 K for 30 min. Then, a gas mixture of 9.5% N_2/CH_4 was admitted into the reactor, which was adjusted through a Brooks mass flow controller at a space velocity of 1500 mL/(g·h). The products were analyzed by an on-line gas chromatograph (Shimadzu GC-9A) equipped with double detectors (both TCD and FID). The use of N_2 as an internal standard enables accurate determination of methane conversion and selectivity of all main products, meanwhile taking into account carbonaceous deposition. The conversion of methane and selectivity of products are calculated according to the carbon number basis.

3. Results and Discussion

3.1. Fresh Catalysts. *^{27}Al MAS and ^{1}H → ^{27}Al CP/MAS NMR.* ^{27}Al MAS NMR is sensitive to the variation of zeolitic construction. Species with different structures or different environments will have a different chemical shift in the ^{27}Al MAS NMR spectra.[31] Figure 1a shows the ^{27}Al MAS NMR of HMCM-22 zeolites with increasing Mo loading. Besides the extraframework octahedral aluminum at 0 ppm, two distinct

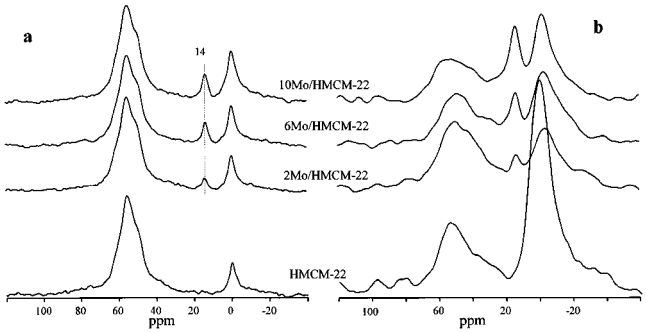

Figure 1. ^{27}Al MAS NMR (a) and the corresponding ^{1}H → ^{27}Al CP/MAS NMR (b) spectra of HMCM-22 with different Mo loadings. Prior to the experiments, the samples were completely hydrated in a desiccator with saturated NH_4NO_3.

components with chemical shifts at 55 and 50 ppm respectively can be clearly resolved in the spectra of HMCM-22 zeolite. At the same time, a line at 60 ppm appeared as a shoulder of the signal at 55 ppm,[38−43] which could be more clearly observed under a very high field spectrometer (17.6 T, Hunger et al.[39] and Lawton et al.[41]). Both these lines belong to framework aluminum. With the increase of the Mo content, one could note that the intensity of the framework aluminum decreased a little, whereas the overall line width of these peaks broadened slightly, but no specific aluminum peak was preferentially reduced; i.e., no framework aluminum attributed to definite *T* site was preferentially expelled from the zeolite lattice.[41] At the same time, the intensity of extraframework octahedral aluminum at 0 ppm got a slight increase. This phenomenon implies that the interaction between the molybdenum species and the framework does exist. It is consistent with our previous observation in which the Al···MoO_x species was found to be formed during the impregnation and calcination processes of the catalyst, leading to the appearance of the superhyperfine structure of the Mo^{5+} signal in the EPR spectra.[17] Meanwhile, this kind of interaction occurs in three different framework aluminum species comparably, since no preferential dealumination was observed as compared with the results of other authors on $SiCl_4$ dealuminated MCM-22 zeolite.[39] They assigned these lines at different chemical shifts to aluminum located at different *T* sites.[41] Thus, molybdenum may interact with aluminum at different *T* sites with a similar manner under the present condition. Moreover, with the introduction of molybdenum, a new peak at 14 ppm can be clearly resolved in the ^{27}Al MAS spectra of HMCM-22 supported Mo catalyst, and the intensity of this peak grows with the increase of Mo loading. This newly appeared peak can be attributed to a hydrated form of an aluminum molybdate ($Al_2(MoO_4)_3$) phase with the tentative formula of $[Al(OH)_n(H_2O)_{6-n}]_n(MoO_4)$, where $n = 1$ or 2,[44] resulting from a full hydration of the sample in a desiccator with saturated NH_4NO_3 before the ^{27}Al MAS and CP/MAS test, whereas the nonhydrated $Al_2(MoO_4)_3$ phase will cause a distinct ^{27}Al resonance at −14 ppm in ^{27}Al MAS NMR spectra, as has been monitored in the HZSM-5 supported Mo catalyst system.[13,16] Apparently, this appearance of the species is resulted from a strong interaction between the molybdenum and the zeolite aluminum species.

^{1}H → ^{27}Al CP/MAS NMR measurement could give the information about aluminum connected with hydroxyl species through observing the relative enhancement of the aluminum signal; i.e., some of the signals will be selectively enhanced in the CP/MAS experiments due to their different extents of interaction with hydroxyls species. The ^{1}H → ^{27}Al CP/MAS NMR spectra of HMCM-22 and Mo/HMCM-22 are presented in Figure 1b. After cross-polarization, the intensity of the signal at 0 ppm, which is assigned to the extraframework aluminum species, is greatly enhanced. It suggests that extraframework aluminum has a close relationship with the proton groups; it probably consists mainly of $[Al(OH)_n]^{3-n}$, $Al(H_2O)_6^{3+}$, etc.[45] With the increase of the Mo loading, the intensity of the resonance is at ca. 60−50 ppm, which is responsible for the framework aluminum's apparent decrease, suggesting that the amount of hydroxyls associating with the framework aluminum reduced with the increase of the Mo loading. The details will be discussed in the following section. At the same time, the peak at about 0 ppm underwent a slight decrease at first and then increased with the increase of Mo loading. This is not hard to imagine: the introduced molybdenum may also have an interaction with the extraframework aluminum species and leads to/catalyzes the condensation of low-molecular-weight aluminum species into polymeric aluminum species,[46] or in another case, direct condensation between the hydroxyl species of molybdenum and nonframework aluminum. They both are responsible for the observed lowering of the cross-polarized efficiency. Further increasing the molybdenum content gave a stronger interaction. Thus, more nonframework aluminum and aluminum molybdate were formed. The selective enhancement of the peak at ca. 14 ppm demonstrated that the corresponding species is a proton-rich species, which supports the assignment of this species to $[Al(OH)_n(H_2O)_{6-n}]_n(MoO_4)$ (originated from hydration of $Al_2(MoO_4)_3$ crystallites).

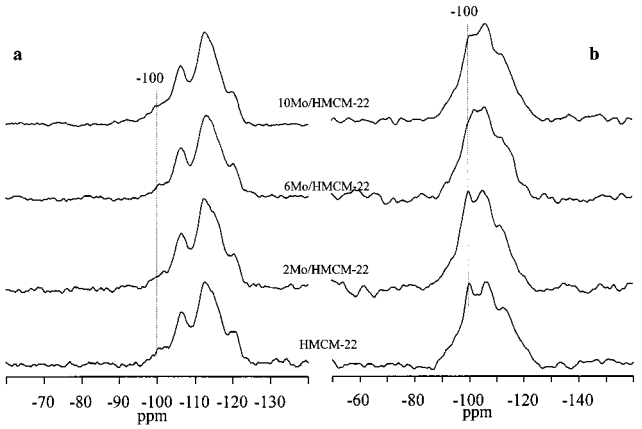

Figure 2. ^{29}Si MAS NMR (a) and the corresponding ^{1}H → ^{29}Si CP/MAS NMR (b) spectra of HMCM-22 with different Mo loadings.

^{29}Si MAS and ^{1}H → ^{29}Si CP/MAS NMR. ^{29}Si MAS NMR spectra and the corresponding ^{1}H → ^{29}Si CP/MAS NMR spectra are shown in Figure 2. Five resonance peaks located at −120.0, −114.7, −112.6, −106.6, and −100.0 ppm, respectively, can be resolved in the ^{29}Si MAS spectrum of HMCM-22. The first four lines are attributed to inequivalent framework T-sites of the zeolite, which correspond to Si(0Al) units and are the characteristic lines for MCM-22.[25,39,42] The line at ca. −100 ppm is supposed to come from the contribution of Si(3Si)OH or Si(1Al) species.[42] In our previous study, we have demonstrated that both possibilities could not be ruled out.[47] Loading with molybdenum does not alter the spectra much. Even for 10Mo/HMCM-22, no distinct difference with the parent zeolite can be noticed. This fact implies that although the molybdenum species has a strong interaction with the zeolite, it does not reach the stage of destroying or changing the zeolite lattice at the present calcination temperature. The ^{1}H → ^{29}Si CP/MAS NMR spectra of HMCM-22 are similar to those reported by

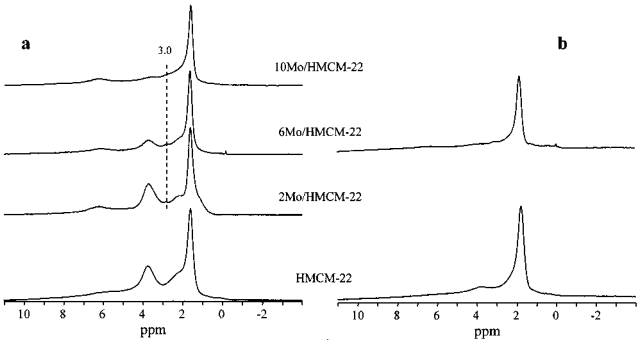

Figure 3. ^{1}H MAS NMR (a) and ^{1}H{^{27}Al} spin echo MAS NMR (b) spectra of HMCM-22 with different Mo loadings. For each spectrum, 200 scans were accumulated. In the spin echo experiments, the spinning speed was set to 5 kHz, and each τ period was equal to one rotor period in the experiments.

Kolodziejski et al.[42] Resonances located at about −100.0 and −106.6 ppm are selectively enhanced with respect to others. Only lines from silanol groups or from the silicon which is closely related to the hydroxyls species would be expected to be enhanced in the ^{1}H → ^{29}Si CP/MAS NMR spectra. So for the present case, the peak at ca. −100.0 ppm comes, at least in part, from the silanol groups. This kind of enhancement is very strong for the HMCM-22 zeolite, while that is less apparent for the Mo/HMCM-22, especially for those with higher molybdenum loading. This may result from the reaction/condensation between the Mo species and the silanol groups. However, the decrease of the enhancement is not as obvious as that in the Mo/HZSM-5 system,[16] which reveals that the interaction of molybdenum with the silanol groups is not as strong as that in the Mo/HZSM-5 catalysts.

^{1}H MAS and ^{1}H{^{27}Al} SEDOR MAS NMR. ^{1}H MAS NMR can provide direct knowledge about the hydroxyl species in catalyst surfaces and has been widely used for the characterization of acidic properties of heterogeneous catalysts.[48] The ^{1}H MAS NMR spectra of HMCM-22 and Mo/HMCM-22 with different Mo loadings are shown in Figure 3. Three peaks centered at about 6.0, 3.7, and 1.6 ppm are present in the ^{1}H MAS NMR spectrum of the HMCM-22 sample, and moreover, a less resolved peak at about 2.2 ppm presents as a shoulder of the peak at 1.6 ppm. The peak at 3.7 ppm can be attributed to bridging OH groups (Brönsted acid sites), while that at 1.6 ppm, which is very intense in the spectra, can be assigned to silanol groups. The feature of the latter is easy to understand: MCM-22 is a thin platelike crystal with an extremely large external surface area[28] and has more terminal silanol groups as compared with other zeolites like ZSM-5. In fact, it has already been verified that nearly all the silanol groups of the as-synthesized HMCM-22 zeolite are terminal Si−OH species.[47] The line at ca. 6.0 ppm is composed of a narrow and a broad peak ascribed to water adsorbed on Lewis sites[49,50] and another kind of Brönsted acid site that interacts electrostatically with the zeolite framework.[51,52] By using the ^{1}H{^{27}Al} SEDOR MAS technique, one can find that the lines located at 6.0, 3.7, and 2.2 ppm are heavily suppressed, while the one at 1.6 ppm remains unchanged (Figure 3b). This is consistent with the assignment that the first three lines are directly connected with the aluminum nuclei. At the same time, the one at ca. 2.2 ppm can be attributed to extraframework Al−OH species. With loading of molybdenum, one may notice that a new peak at ca. 3.0 ppm appeared. It becomes more apparent when the intensity of the Brönsted acid sites at 3.7 ppm and the extra-lattice Al−OH at 2.2 ppm decrease (see the upper two lines in Figure 3a). With Al irradiation, this species seems not to change (see Figure 3b). This fact implies that this hydroxyl group is not directly coupled with aluminum, or its distance to aluminum is longer than 4 Å. Probably, it comes from the hydrogen-bonded metal OH groups (for example MoOH), which have been reported by Hunger et al.[48,53] But this needs further clarification, such as by the use of ^{1}H{^{95}Mo} spin echo double resonance since molybdenum is also a quadrupolar nuclear.

After the introduction of molybdenum, it is apparent from ^{1}H MAS NMR spectra in Figure 3a that the overall proton signal intensity decreases with the increase of molybdenum loading. These facts reveal that the condensation/reaction between the molybdenum species and the hydroxyl species of HMCM-22 happened in the impregnation and calcination processes of the catalysts. This is in good agreement with our previous conclusion from EPR[17] and the results of Borry III et al. for monitoring the water desorption in the solid-state reaction during the preparation of the catalyst.[14] Among the hydroxyl species, it should be noted that shrinking of the silanol group (at ca. 1.6 ppm) of the HMCM-22 after loading molybdenum is not so obvious as those taking place on its Brönsted acid sites (ca. 3.7 and 6.0 ppm) or extra-lattice Al−OH (ca. 2.2 ppm). Nevertheless, in the case of Mo/HZSM-5 catalysts, the silanols of the HZSM-5 are preferentially reacted with molybdenum species, for example, for 10Mo/HZSM-5, there were only 2% silanol groups retained as compared with the parent HZSM-5, whereas about one-fourth of the Brönsted acid proton remained with respect to the parent zeolite.[54] These phenomena strongly indicated that the interaction between molybdenum and aluminum is more pronounced in Mo/HMCM-22 than in Mo/HZSM-5, which may give rise to the formation of a larger amount of Mo−O−Al groups with the release of protons in the zeolitic OH group as compared with Mo/HZSM-5. As most of the Brönsted acid sites are located at the internal channels of HMCM-22 (>75%), while most of the silanol groups stay at the external surface,[47] it suggests that molybdenum is better distributed on the *internal* zeolitic channels of HMCM-22, as judged by its preferential reaction with the Brönsted acid sites, whereas a relatively larger amount of molybdenum is located on the external surface of HZSM-5 in the Mo/HZSM-5 system. This may be attributed to the different channel structures that the MCM-22 zeolite possessed: there are a great number of 12-member ring supercages in one of its channel systems that connect with each other through the ten-ring windows.[27,28] The greater surface area of MCM-22 (about 500 m^2/g) as compared with HZSM-5 (about 350 m^2/g) originates from this kind of structure. The large number of supercages together with the Brönsted acid site therein (which may serve as a powerful trap for the migration of molybdenum) enables the accommodation of more molybdenum in the internal channel system. The interaction between Mo and Brönsted aluminum also results in a line-broadening effect in the framework Al region of the ^{27}Al MAS NMR spectra, as well as in a decrease of the intensity of the peak at about 50−60 ppm in ^{1}H → ^{27}Al CP/MAS experiments, since the CP source−Brönsted protons associated with these aluminums are replaced by molybdenum (Figure 1). And if this kind of interaction is strong enough, it would lead to the expelling of framework aluminum, and as a consequence, extra-lattice aluminum or $Al_2(MoO_4)_3$ would be formed. However, at the present situation, this effect has not reached the stage of influencing the stability of the zeolite lattice, as has been verified by the ^{29}Si MAS NMR, ^{27}Al MAS, and ^{1}H → ^{27}Al CP/MAS NMR experiments in the above section. Details about how and when the interaction occurs between the Mo

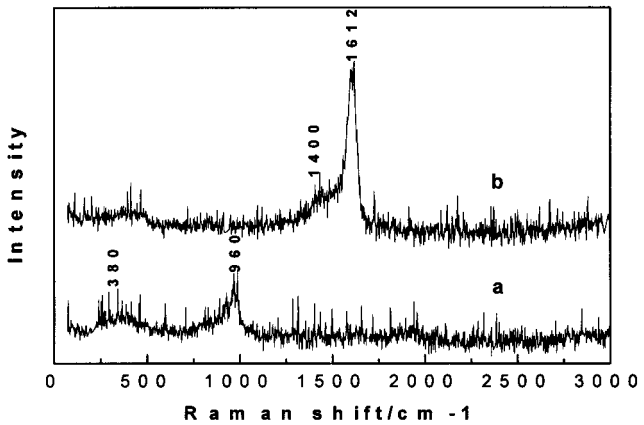

Figure 4. UV−Raman spectra of fresh (a) and coked (b) (6 h reaction) 6Mo/HMCM-22 catalysts.

and the zeolites, and which factors govern this kind of interaction need further investigation.

3.2. Used Catalysts. *UV−Raman Spectroscopy.* UV−Raman spectroscopy can effectively avoid the influence of fluorescence; therefore, it is possible to investigate some important issues of catalysis.[37,55] Figure 4 displays the UV−Raman spectra of the fresh 6Mo/MCM-22 and the deactivated catalyst. For the fresh 6Mo/HMCM-22, two bands at 950 cm^{-1} and about 350−380 cm^{-1} are observed. The former (with a shoulder at downshift) can be attributed to the Mo═O stretch, while the latter at 350−380 cm^{-1} is due to the characteristic band of the zeolite or Mo═O bending modes.[56] After deactivation of the catalyst, these bands disappeared, indicating that the reduction of the molybdate occurred or the carbonaceous deposits hindered the detection of the signals of the catalyst. Meanwhile, a big band at 1612 cm^{-1} appears with a shoulder at about 1400 cm^{-1}, both of which come from the coke species.[55] Absence of the band at about 3000 cm^{-1} suggests that the coke is not a hydrogen-rich paraffinic coke species. The 1612 cm^{-1} band is due to the C═C stretching mode and can be ascribed to aromatic carbon deposits.[57] The shoulder at about 1400 cm^{-1} seems to come from the C−H bending mode of graphite or quasi-graphite species. This is in good agreement with the fact that we cannot get the $^{1}H \rightarrow {}^{13}C$ CP/MAS NMR spectra of the used catalysts even if 15 000 scans are accumulated, which strongly suggests that the coke is a hydrogen-deficient type. This has also been suggested by Lunsford et al. in their XPS study.[58]

^{29}Si MAS and $^{1}H \rightarrow {}^{29}Si$ CP/MAS NMR. The ^{29}Si MAS and $^{1}H \rightarrow {}^{29}Si$ CP/MAS NMR spectra of the 6Mo/HMCM-22 (which is the optimum Mo loading for the reaction; see the following section) with various reaction times are shown in Figure 5. After reaction at 973 K for 30 min, the line width of the Si(0Al) sites at −120.0, −114.7, −112.6, and −106.6 ppm were broadened. As a result, the splitting between these lines was overlapped and less clear. This trend becomes more obvious with prolongation of the reaction time, i.e., for the ^{29}Si MAS NMR spectrum of the 6Mo/HMCM-22 after 6 h reaction, only the peak at −112.6 ppm can be clearly resolved. The lines at −100.0 and −120.0 ppm became a shoulder of that main peak, and the one at −114.7 ppm already disappeared. Meinhold et al.[59] had investigated the influence of coke on the ^{27}Al and ^{29}Si MAS NMR spectra of HZSM-5. They found that the ^{29}Si peak would shift upfield at the same time with line broadening. These phenomena are similar to the template-containing zeolite system. With this consideration, they tentatively ascribed the former to the preferential restriction of accession of oxygen to certain Si sites by coke and the latter to the distortion of the zeolitic

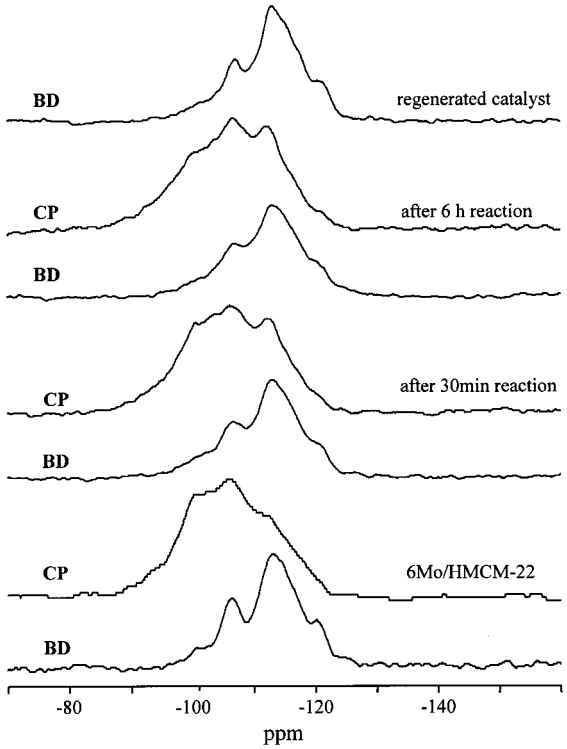

Figure 5. ^{29}Si MAS NMR and the corresponding $^{1}H \rightarrow {}^{29}Si$ CP/MAS NMR spectra of 6Mo/HMCM-22 (which has the most suitable Mo loading) with various reaction time.

channel wall by a bulkier and more rigid molecule. In the present case, we do not observe a peak shift. The line broadening here is probably similar to their conclusion: the interaction between the zeolite channels and the coke species does exist, and it will result in a dipole−dipole broadening effect of the specific Si atom. With the increase of time on stream, the coke contents will become larger, and hence, a stronger interaction between the coke and the Si atom will occur. In common case, the CP effect in $^{1}H \rightarrow {}^{29}Si$ CP/MAS of the coked sample comes from the protons in carbonaceous species. The hydrogen content in the coked sample could be calculated from the intensity of its CP/MAS spectra by taking the CP/MAS intensity of the zeolite sorbed with different amounts of benzene as an external standard.[59] However, this method seems to be unsuitable for the current case. The enhancement of the silanol group is similar to or larger than that of other sites, which indicates that the CP tools of the samples come from both the remaining silanol groups and the coke species (Figure 5), especially those with a small amount of coke, such as in the case of the sample after 30 min reaction. If the cross-polarization only comes from the hydrogen in the coke species, one would not observe the selective enhancement of the peak at −100.0 ppm. In fact, there are two possibilities for the observed double-CP tool. The first is that during the reaction, hydroxyl species such as silanol groups are properly kept, and the second possibility is that the content of hydrogen in the coke is so small that it is comparable with the amount of hydroxyls species. We believe that both possibilities hold, for as we have mentioned previously, there is a large amount of silanol groups in MCM-22 and the carbonaceous deposits on this catalyst are a hydrogen-deficient type. With the increase of reaction time, the ratio of the intensity of the peak at −112.6 ppm to that at −100.0 ppm increases, indicating that the contribution from coke becomes dominant (the increase of coke content). Another interesting feature is that the ratio of intensity of the peak at −112.6 ppm to that at

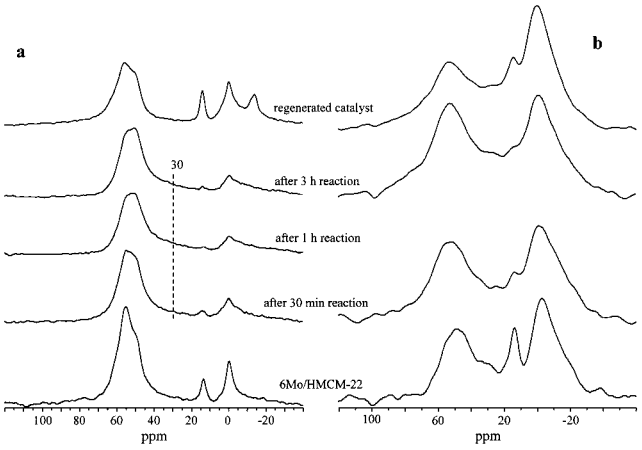

Figure 6. ^{27}Al MAS NMR (a) and the corresponding ^{1}H → ^{27}Al CP/MAS NMR (b) spectra of 6Mo/HMCM-22 with various reaction time and regeneration. The regeneration of the coked catalyst was carried out in a 15% O_2/N_2 (50 mL/min) stream at 793 K.

−120.0 ppm in the coked sample is larger than that on the ^{29}Si MAS spectra. This may suggest that coke is preferentially deposited on the sites linked with the peak at −112.6 ppm, whereas sites at −120.0 ppm have less probability of contaction with the reaction molecule.

^{27}Al MAS and ^{1}H → ^{27}Al CP/MAS NMR. After reaction, a significant change can be found in the ^{27}Al MAS NMR spectra (Figure 6). Among the three framework aluminum peaks of the parent MCM-22, the one at 55 ppm is the highest. By careful analysis, Lawton et al.[41] suggested that the corresponding T1, T3, T4, T5 and T8 sites are aluminum-enriched. However, after half an hour reaction, the intensity of the peak decreased as compared with the other (two) peaks. With prolongtion of the reaction, this trend continued, but not as apparent as what happened in the first half-hour. Moreover, the line width of these peaks broadens, and there appears a new peak at about 30 ppm, which is due to nonframework four-coordinated aluminum species that released from the zeolite lattice.[60] As reported by Meinhold et al.,[59] the changes in ^{27}Al spectra can be ascribed to the displacement of water and oxygen by the coke in the channels, and therefore, it increases the electric-field gradient around aluminum. As a result, the line broadening due to T2 broadening would be expected. In addition, the employment of a higher reaction temperature (973 K) also causes line broadening. At that temperature, the interaction between the molybdenum and framework aluminum is enlarged, and consequently, leads to the distortion of the zeolite lattice. If this kind of interaction becomes more severe, the formation of the nonframework 4-coordinated aluminum at about 30 ppm is observed. It will increase with the time on stream. Meanwhile, the formation of this species may also be originated from coke deposition, as in the case of coked HY catalyst.[61] Both of the reasons mentioned are responsible for this phenomenon, since the catalyst here is a Mo-modified zeolite other than one-component catalysts. On the other hand, the intensity of the peak at 14 ppm attributed to $[Al(OH)_n(H_2O)_{6-n}]_n(MoO_4)$ decreases with the reaction time, and it almost disappears after 3 h of reaction. This fact suggests that the part of the coke is formed on or in the $Al_2(MoO_4)_3$ crystallites during the reaction, and it is the connection of this species with coke that hinders the rehydration of its own. Interestingly, no peak at about −14 ppm can be resolved in the coked sample. However, we notice that after coking, a shoulder appeared in the high field part of the signal associated with 0 ppm extraframework octahedral aluminum. It probably results from the coked-$Al_2(MoO_4)_3$ species, the symmetry of which is heavily distorted by coke in the reaction process and similar to the amorphous aluminum molybdate reported by Han and co-worker.[62]

A dramatic change occurred after regeneration of the coked catalyst (6 h reaction) by flowing oxygen at 773 K. The intensity of the peak attributed to nonframework octahedral aluminum increases at the same time of reappearing of the peak at 14 ppm and advent of an additional peak at ca. −14 ppm. Meanwhile, nonframework 4-coordinated aluminum (at about 30 ppm) almost disappeared. We may deduce that it has transformed into the aluminum species in the high-field region (those at 14, 0, and −14 ppm) with the help of molybdenum, since it was reported that molybdate is more active or easier to move/sublimate in an oxygen atmosphere at high temperature, which promotes the reaction of Mo with the aluminum.[14] The restoration of a peak at 14 ppm can be attributed to the burning-off of carbonaceous deposits during regeneration, which hinder the rehydration of aluminum molybdate into the $[Al(OH)_n(H_2O)_{6-n}]_n(MoO_4)$ phase. However, the appearance of the 14 ppm peak seems rather interesting. If a similar case that happened on the Mo/HZSM-5 holds,[16] the $Al_2(MoO_4)_3$ crystallites at −14 ppm here would be easy to hydrate into the $[Al(OH)_n(H_2O)_{6-n}]_n(MoO_4)$ phase (at 14 ppm), since the time in which this regenerated catalyst stayed in the desiccator was the same as that of the other catalysts. However, the coexistence of these two phases ($Al_2(MoO_4)_3$ crystallites and $[Al(OH)_n(H_2O)_{6-n}]_n(MoO_4)$ phase) is observed in this case. As pointed out by Han et al.,[62] the rehydration of the $Al_2(MoO_4)_3$ on the catalyst surface is easy to carry out while that in the bulk phase is more difficult. Maybe, a bulkier $Al_2(MoO_4)_3$ crystallite is formed during regeneration (in oxygen atomsphere) of coked Mo/HMCM-22, which is not easy to be hydrated.

Information about the location of the coke can be given by the ^{27}Al CP/MAS experiments, since the cross-polarization comes, at least in part, from the proton in the carbonaceous deposits. After reaction, the peak at 50−60 ppm is preferentially enhanced (Figure 6b). With the prolongtion of the reaction, it will reach an equal intensity with the nonframework aluminum at ca. 0 ppm. Meanwhile, no clear peak at 30 ppm can be resolved, although the formation of this species is obviously observed in ^{27}Al MAS NMR spectra. This fact indicates that the enhancement of this species is not as obvious as that of the framework aluminum at about 50−60 ppm in the ^{1}H → ^{27}Al CP/MAS NMR experiments. Both of these results show that most of the coke deposits occur on the framework aluminum sites (Brönsted site). In addition, the redecrease of this peak in the regenerated sample strongly argues this conclusion.

^{27}Al MAS NMR spectra of the 2Mo/HMCM-22 and 10Mo/HMCM-22 before and after 3 h reaction at 973 K are shown in Figure 7. One can note that similar to the 6Mo/HMCM-22, part of the framework aluminum at ca. 55 ppm is preferentially expelled from the lattice. However, a significant change happened in the 10Mo/HMCM-22 after reaction: the intensity of framework Al greatly reduced, which indicates that a large amount of aluminum has been released from the zeolite lattice. As already shown in the above section (proton MAS NMR), during the preparation process of Mo/HMCM-22, molybdenum may migrate into the internal channels of the zeolite and substitute the protons of the Brönsted acid sites. The higher the molybdenum content, the more the Al−O−Mo species would be formed. At the same time, redundant molybdenum would heavily distort the lattice of the zeolite, and will extract Al from it when a high treating temperature is experienced.[13,63] Thus, it

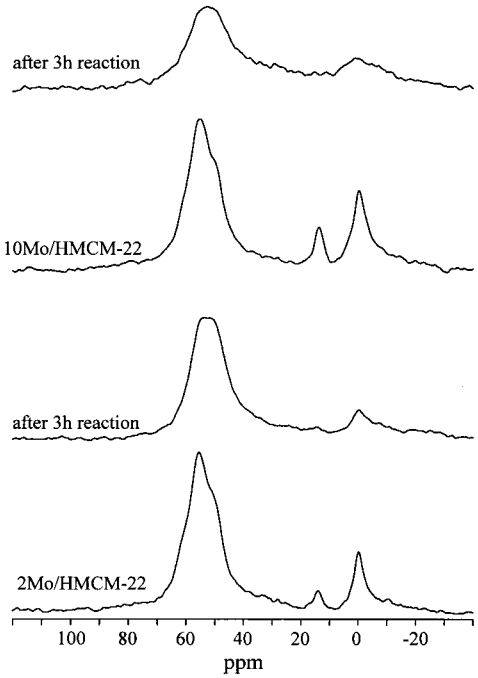

Figure 7. ^{27}Al MAS NMR spectra of fresh and coked 2Mo/HMCM-22 (a) and 6Mo/HMCM-22 (b) catalysts.

is not difficult to understand the poor catalytic performance of the 10Mo/HMCM-22, which will be discussed below.

3.3. Catalyst Evaluation and General Discussion. The catalytic performances of various samples are listed in Table 1. It is interesting to find that 6Mo/HMCM-22 is much better than the others. Both the conversion of methane and selectivity of benzene are the highest, while the selectivity to coke is the lowest. After regeneration, the catalytic performance can be properly recovered, only with a slight decrease in methane conversion. It can be well explained if sublimation of Mo during the oxygen regeneration is considered.

As reported in previous studies, the Mo-modified zeolite catalysts for methane dehydro-aromatization are bifunctional catalysts. The initial methane activation is realized on Mo (Mo_2C) sites, whereas the succeeding aromatization of intermediate species, i.e., ethene, ethane, or the so-called "carbon pool",[5,7,8,11] occurs on the acidic sites, especially on Brönsted acid sites. A good catalytic performance could be expected only if a good cooperation between these two sites is established. The present results reveal that an interaction between molybdenum and the zeolite lattice exists. During the impregnation and calcination processes, Mo would closely contact with the aluminum species in the zeolite, particularly with framework aluminum. At the same time, Brönsted acid sites may serve as a powerful trap for the migration of molybdenum into the internal channels. As a result, molybdenum is anchored at the Brönsted aluminum and Mo−O−Al groups are formed. These lead to not only a good dispersion of molybdenum but also the reduction of hydroxyl species. Both the ^{27}Al MAS and ^{1}H MAS NMR spectra suggest that, for MCM-22, molybdenum reacts preferentially with Brönsted acid sites (framework aluminum), while it will preferentially interact with silanol groups (in external surface) in the case of ZSM-5. It implies that molybdenum will be better distributed in the internal channels of MCM-22 due to the unique structure of MCM-22. With the 12-ring supercages, MCM-22 can accommodate more transition metal ions. As indicated in the proton MAS NMR experiments, only a small portion of the Brönsted acid sites are retained for high Mo loading catalysts as compared with the parent HMCM-22 zeolite. However, an optimal value may be required for the collaboration between the dispersion of molybdenum and the number of Brönsted acid sites remained, because they have, actually, a close relationship with each other. Moreover, as is well-known, the reactions are conducted at 973 K while the catalyst is calcinated at 773 K. The interaction between aluminum and molybdenum would become stronger in the former case, as demostrated by ^{27}Al MAS NMR spectra of used catalyst; i.e, at that temperature, it leads to a more severe distortion and weakening of the zeolite lattice, and consequently, partial dealumination happened for the 6Mo/HMCM-22 catalyst. But in the case of the 10Mo/HMCM-22, this interaction is so strong that a large amount of aluminum would be expelled from the zeolite lattice. Thus, it is easy to imagine the poor catalytic performance of the 10Mo/HMCM-22, as listed in Table 1. Another possibility is that the limited Brönsted acid sites of 10Mo/HMCM-22 cannot accomplish the smooth aromatization of activated carbon species, and thus, hinder the continuous transformation of methane. We believe that the former is more reasonable, since we do observe the destruction of the zeolite lattice after reaction. However, 2Mo/HMCM-22 is also not a good catalyst. Probably, it is due to its low Mo loading, so that there are not enough molybdenum sites for initial methane activation. The proper combination of molybdenum and residual Brönsted acid sites in the 6Mo/HMCM-22 catalyst is responsible for its outstanding catalytic performance.

A small portion of framework aluminum would transform into nonframework 4-coordinated aluminum by the action of molybdenum in the reaction process (see Figure 6). In an oxygen atmosphere (in regeneration), it reacts with the nearby molybdenum to form $Al_2(MoO_4)_3$ crystallites (the fresh catalyst also contain small amount of such species originated from calcination at 773 K). This species has been taken as the detrimental material in the Mo/HZSM-5 catalyst system, which is responsible for the inferior catalytic performance of high temperature calcinated or nanosized zeolite-supported catalyst.[13,16,63] However, the present results indicate that although the regeneration of the catalyst leads to the formation of considerable amount of $Al_2(MoO_4)_3$ crystallites, the yield of aromatic products are properly restored. This suggests that if the amount of remaining framework aluminum/Brönsted sites are sufficient for accomplishing the aromatization of the intermediates, the activity of the catalyst would not be heavily influenced. Maybe, it is the destruction of the zeolite lattice that results in the bad catalytic performance, which is, to some extent, similar to what happened in 10Mo/HMCM-22 at 973 K.

Acknowledgment. We are very grateful to the support of the National Natural Science Foundation of China and the Ministry of Science and Technology of China, and to Prof. Can Li and Mrs. Meijun Li for their kind help in UV-Raman experiments.

References and Notes

(1) Crabtree, R H. *Chem. Rev.* **1995**, *95*, 987.

(2) Axelrod, M. G.; Gaffney, A. M.; Pitchai, R.; Sofranko, J. A. In *Natural Gas Conversion II*; Curry-Hyde, H. E., Howe, R. F., Eds.; Elsevier: New York, 1994; p 93.

(3) Periana, R. A.; Taube, D. J.; Evitt, E. R.; Löffler, D. G.; Wentrcek, P. R.; Voss, G.; Matsuda, T. *Science* **1993**, *259*, 340.

(4) Lunsford, J. H. *Stud. Surf. Sci. Catal.* **1993**, *75*, 103.

(5) Wang, L.; Tan, L.; Xie, M.; Xu, G.; Huang, J.; Xu, Y. *Catal. Lett.* **1993**, *21*, 35. Xu, Y.; Liu, S.; Wang, L.; Xie, M.; Guo, X. *Catal. Lett.* **1995**, *30*, 135. Shu, Y.; Xu, Y.; Wong, S.; Wang, L.; Guo, X. *J. Catal.* **1997**, *179*, 11.

(6) Wang, D.; Lunsford, J. H.; Rosynek, M. P. *Top. Catal.* **1996**, *3*, 289.
(7) Wang, D.; Rosynek, M. P.; Lunsford, J. H. *J. Catal.* **1997**, *169*, 347.
(8) Solymosi, F.; Erdöhelyi, A.; Szöke, A. *Catal. Lett.* **1995**, *32*, 43. Solymosi, F. *Appl. Catal. A Gen.* **1996**, *142*, 361.
(9) Solymosi, F.; Szöke, A.; Cserényi, J. *Catal. Lett.* **1996**, *39*, 157. Solymosi, F.; Cserényi, J.; Szöke, A.; Bansagi, T.; Oszkó, A. *J. Catal.* **1997**, *165*, 150.
(10) Solymosi, F.; Bugyi. L.; Oszkó, A. *Catal. Lett.* **1999**, *57*, 103.
(11) Schuurman, Y.; Decamp, T.; Pantazidis, A.; Xu, Y D.; Mirodatos, C. *Stud. Surf. Sci. Catal.* **1997**, *109*, 351.
(12) Liu, S.; Dong, Q.; Ohnishi, R.; Ichikawa, M. *Chem. Commun.* **1998**, 1217. Liu, S.; Wang, L.; Ohnishi, R.; Ichikawa, M. *J. Catal.* **1999**, *181*, 175. Ohnishi, R.; Liu, S.; Dong, Q.; Wang, L.; Ichikawa, M. *J. Catal.* **1999**, *182*, 92.
(13) Zhang, J. Z.; Long, M. A.; Howe, R. F. *Catal. Today* **1998**, *44*, 293.
(14) Borry, R. W., III; Kim, Y. H.; Huffsmith, A.; Reimer, A.; Iglesia, I. *J. Phys. Chem. B* **1999**, *103*, 5787.
(15) Mériaudeau, P.; Ha, V. T. T.; Tiep, L. V. *Catal. Lett.* **2000**, *64*, 49.
(16) Zhang, W.; Ma, D.; Han, X.; Liu, X.; Bao, X.; Guo, X.; Wang, X. *J. Catal.* **1999**, *188*, 393.
(17) Ma, D.; Shu, Y.; Bao, X.; Xu, Y. *J. Catal.* **2000**, *189*, 314.
(18) Solymosi, F.; Bugyi, L.; Oszko, A.; Horvath, I. *J. Catal.* **1999**, *185*, 160.
(19) Kim, Y.; Borry, R. W., III; Iglesia, E. *Microporous Mesoporous Mater.* **2000**, *35*−*36*, 495.
(20) Ma, D.; Shu Y.; Zhang, W.; Han, W.; Xu, Y.; Bao, X. *Angew. Chem., Int. Ed. Engl.* **2000**, *39*, 2928. Ma, D.; Shu Y.; Cheng, M.; Xu, Y.; Bao, X. *J. Catal.* **2000**, *194*, 105.
(21) Wang, L.; Ohnishi, R.; Ichikawa, M. *Catal. Lett.* **1999**, *62*, 29.
(22) Wang, L.; Ohnishi, R.; Ichikawa, M. *J. Catal.* **2000**, *190*, 276.
(23) Shu, Y.; Ma, D.; Xu, L.; Xu, Y.; Bao, X. *Catal. Lett.*, in press.
(24) Leonowicz, M. E.; Lawton, J. A.; Lawton, S. L.; Rubin, M. K. *Science* **1994**, *264*, 1910.
(25) Kennedy, G. J.; Lawton, S. L.; Rubin, M. K. *J. Am. Chem. Soc.* **1994**, *116*, 11000.
(26) Nicolopooulos, S.; González-Calbet, J. M.; Vallet-Regí, M.; Corma, A.; Corell, C.; Guil, J. M.; Pérez-Pariente, J. *J. Am. Chem. Soc.* **1995**, *117*, 8947.
(27) Corma, A.; Corell, C.; Pérez-Pariente, J. *Zeolites* **1995**, *15*, 2.
(28) Lawton, S. L.; Leonowicz, M. E.; Partridge, R. D.; Chu, P.; Rubin, M. K. *Microporous Mesoporous Mater.* **1998**, *23*, 109.
(29) Corma, A. *Microporous Mesoporous Mater.* **1998**, *21*, 487.
(30) Del Rossi, K. J.; Huss, A., Jr. U.S. Patent 5 107 047, 1992. Corma, A.; Corell, C.; Flopis, F.; Martínez, A.; Pérez-Pariente, J. *Appl. Catal. A: General* **1994**, *115*, 121. Verhoef, M. J.; Creyghton, E. J.; Peters, J. A.; van Bekkum, H. *Chem. Commun.* **1997**, 1989. Wu, P.; Komatsu, T.; Yashima, T. *Microporous Mesoporous Mater.* **1998**, *22*, 343. Corma, A.; Martínez-Triguero, J. *J. Catal.* **1997**, *165*, 102.
(31) Bell, A. T.; Pines, A. *NMR Techniques in Catalysis*; Dekker: New York, 1994.
(32) Rocha, J.; Carr, S. W.; Klinowski, J. *Chem. Phys. Lett.* **1991**, *187*, 401.
(33) Rocha, J.; Liu, X.; Klinowski, J. *Chem. Phys. Lett.* **1991**, *182*, 531.
(34) Zhang, W.; Ma, D.; Liu, X.; Liu, X.; Bao, X. *Chem. Commun.* **1999**, 1091.
(35) van Eck, E. R. H.; Janssen, R.; Mass, W. E. J. R.; Veeman, W. S. *Chem. Phys. Lett.* **1990**, *174*, 428.
(36) Zeng, Q.; Nekvasil, H.; Grey, C. P. *J. Phys. Chem. B* **1999**, *103*, 7406.
(37) Li, C.; Xiong, G.; Xin, Q.; Liu, J.; Ying, P.; Feng, Z.; Li, J.; Yang, W.; Wang, Y.; Wang, G.; Liu, X.; Lin, M.; Wang, X.; Min, E. *Angew. Chem., Int. Ed. Engl.* **1999**, *15*, 2220.
(38) Unverricht, S.; Hunger, M.; Ernst, S.; Karge, H. G.; Weitkamp, J. *Stud. Surf. Sci. Catal.* **1994**, *84*, 37.
(39) Hunger, M.; Ernst, S.; Weitkamp, J. *Zeolites* **1995**, *15*, 188.
(40) Ravishankar, R.; Sen, T.; Sivasanker, S.; Ganapathy, S. *J. Chem. Soc., Faraday Trans.* **1995**, *91*, 3549.
(41) Lawton, S. L.; Fung, A. S.; Kennedy, G. J.; Alemany, L. B.; Chang, C. D.; Hatzikos, G. H.; Lissy, D. N.; Rubin, M. K.; Timken, H. C.; Steuernagel, S.; Woessner, D. E. *J. Phys. Chem.* **1996**, *100*, 3788.
(42) Kolodziejski, W.; Zicovich, C.; Corell, C.; Pérez-Pariente, J.; Corma, A. *J. Phys. Chem.* **1995**, *99*, 7002.
(43) Mériaudeau, P.; Tuel, A.; Vu, T. T. H. *Catal. Lett.* **1999**, *61*, 89.
(44) Edwards, J. C.; Decanio, E. C. *Catal. Lett.* **1993**, *19*, 121.
(45) Klinowski, J.; Fyfe, C. A.; Gobbi, G. C. *J. Chem. Soc., Faraday Trans.* **1985**, *81*, 3003.
(46) Campbell, S. M.; Bibby, D. M.; Coddington, J. M.; How, R. F.; Meinhold, R. H. *J. Catal.* **1996**, *161*, 338.
(47) Ma, D.; Deng, F.; Fu, R.; Han, X.; Bao, X. *J. Phys. Chem. B*, in press.
(48) Hunger, M. *Catal. Rev.-Sci. Eng.* **1997**, *39*, 345.
(49) Hunger, M.; Freude, D.; Pfeifer, H. *J. Chem. Soc., Faraday Trans.* **1991**, *87*, 657.
(50) Deng, F.; Du, Y.; Ye, C.; Wang, J.; Ding, T.; Li, H. *J. Phys. Chem.* **1995**, *99*, 15208.
(51) Brunner, E.; Beck, K.; Heeribout, L.; Karge, H. G. *Microporous Mater.* **1995**, *3*, 395.
(52) Beck, L. W.; Haw, J. F. *J. Phys. Chem.* **1995**, *99*, 1076.
(53) Hunger, M.; Freude, D.; Pfeifer, H.; Prager, D.; Reschetilowski, W. *Chem. Phys. Lett.* **1989**, *163*, 221.
(54) Ma, D.; Zhang, W.; Shu, Y.; Xu, Y.; Bao, X. *Catal. Lett.* **2000**, *66*, 155.
(55) Li, C.; Stair, P. C. *Stud. Surf. Sci. Catal.* **1997**, *105*, 599.
(56) Mestl, G. *Catal. Rev. Sci. Eng.* **1998**, *40*, 451.
(57) Li, J. Master Thesis, Dalian Institute of Chemical Physics, CAS, 1999.
(58) Weckhuygen, B. M.; Rosynek, M. P.; Lunsford, J. H. *Catal. Lett.* **1998**, *52*, 31.
(59) Meinhold, R. H.; Bibby, D. M. *Zeolites* **1990**, *10*, 146.
(60) Engelhardt, G.; Michel, D. *High-resolution Solid-State NMR of Silicates and Zeolites*; John Wiley & Sons: Chichester, U.K., 1987.
(61) Bonardet, J. L.; Barraage, M. C.; Fraissard, J. P. In *Proceedings of the 9th International Zeolite Conference Vol. II*; Von Ballmoss, R., et al., Eds.; Butterworth-Heinemann: London, 1993; p 475.
(62) Han, O. H.; Lin, C. Y.; Haller, G. L. *Catal. Lett.* **1992**, *14*, 1.
(63) Liu, W.; Xu, Y.; Wong, S.-T.; Wang, L.; Qiu, J.; Yang, N. *J. Mol. Catal. A: Chem.* **1997**, *120*, 257.